https://doi.org/10.5194/acp-2019-167
Preprint. Discussion started: 7 June 2019

Atmospheric Chemistry and Physics Discussions

Characterization of the radiative impact of aerosols on CO_2 and energy fluxes in the Amazon deforestation arch using Artificial Neural Networks

Renato Kerches Braghiere[1,2,3†], Marcia Akemi Yamasoe[3], Nilton Manuel Evora do Rosário[4], Humberto Ribeiro da Rocha[3], José de Souza Nogueira[5], Alessandro C. de Araújo[6,7]

[1]Jet Propulsion Laboratory, California Institute of Technology, 4800 Oak Grove Drive, Pasadena, CA, 91109, USA

[2]Joint Institute for Regional Earth System Science and Engineering, University of California at Los Angeles, Los Angeles, CA, 90095, USA

[3]Departamento de Ciências Atmosféricas, Instituto de Astronomia, Geofísica e Ciências Atmosféricas, Universidade de São Paulo, São Paulo, Brazil

[4]Universidade Federal de São Paulo, Diadema, Brazil

[5]Instituto de Física, Universidade Federal de Mato Grosso, Mato Grosso, Brazil

[6]Embrapa Amazônia Oriental, Travessa Dr. Enéas Pinheiro, s/n, Marco, Caixa Postal 48, Belém, Pará 66095-100, Brazil.

[7]Instituto Nacional de Pesquisas da Amazônia (INPA), Large Scale Biosphere-Atmosphere Experiment in Amazonia (LBA), Avenida André Araújo, 2936, Manaus, Amazonas, 69060-001, Brazil.

Correspondance to: Renato K. Braghiere (renato.braghiere@gmail.com)

†Current address: NASA Jet Propulsion Laboratory, M/S 233-305F, 4800 Oak Grove Drive, Pasadena, CA, 91109, USA

Abstract. In vegetation canopies with complex architectures, diffuse solar radiation can enhance carbon assimilation through photosynthesis because isotropic light is able to reach deeper layers of the canopy. Although this effect has been studied in the past decade, the mechanisms and impacts of this enhancement over South America remain poorly understood. Over the Amazon deforestation arch large amounts of aerosols are released into the atmosphere due to biomass burning, which provides an ideal scenario for further investigation of this phenomenon in the presence of canopies with complex architecture. In this paper, the relation of aerosol optical depth and surface fluxes of mass and energy are evaluated over three study sites with Artificial Neural Networks and radiative transfer modeling. Results indicate a significant effect of the aerosol on flux of carbon dioxide between the vegetation and the atmosphere, as well as on energy exchange, including that surface fluxes are

https://doi.org/10.5194/acp-2019-167
Preprint. Discussion started: 7 June 2019

Atmospheric Chemistry and Physics Discussions

sensitive to second order radiative impacts of aerosols on temperature, humidity, and friction velocity. CO_2 exchanges increased in the presence of aerosol in up to 55% in sites with complex canopy architecture. A decrease of approximately 12% was observed for a site with shorter vegetation. Energy fluxes were negatively impacted by aerosols over all study sites.

1 Introduction

The composition of the atmosphere is determined by the emission and transport of gases and aerosols at different scales, chemical and microphysical processes, wet and dry deposition, or by the distribution of the land surface and oceanic ecosystems around the globe. These processes are represented by the biogeochemical cycle and they involve interactions between different components of the Earth system. These interactions are generally non-linear and might produce negative or positive radiative forcing signals in the climate system (Forster et al., 2007). The state of the climate system is governed by the energy balance, which is defined as the amount of energy going into the climate system minus the amount of energy dissipated by it mostly through the emission of long wave radiation. In the long term, the amount of solar radiation absorbed by Earth's atmosphere and surface is balanced out by the same amount of longwave radiation emitted by them. About half of the solar radiation is absorbed by the Earth's surface. This energy is transferred to the atmosphere by heating the air in contact with the surface, through evapotranspiration and longwave radiation emission, which can be absorbed by clouds and greenhouse gases. The atmosphere in turn emits longwave energy back to the surface as well as to the space (Kiehl and Trenberth, 1997).

The Earth's climate system has undergone a number of changing processes considered 'natural' throughout the history of the planet. The average temperature of the planet has always been directly linked to the amount of CO_2 in the atmosphere. The uncertainties on the energy balance associated with greenhouse gases have been reduced over the past years; however, uncertainties associated with atmospheric aerosols remain substantial, despite the various advances achieved since the first studies relating aerosols and the climate system (Boucher et al., 2013). Aerosols are technically defined as solid or liquid particles suspended in the air (Seinfeld and Pandis, 2006), that can be emitted from natural or anthropogenic sources. They can be found in different shapes and chemical composition, which may vary according to their source of emission and/or processes they are subjected once in the atmosphere. They can also be classified into primary, i.e., when they are directly emitted, or secondary, i.e., when they are formed in the atmosphere through a physical-chemical process known as gas-particle conversion. The typical diameter of aerosols ranges from a few nanometers to tens of micrometers (Seinfeld and Pandis, 2006) and it can impact their time spent in the atmosphere and their ability to interact with radiation.

https://doi.org/10.5194/acp-2019-167
Preprint. Discussion started: 7 June 2019

Atmospheric Chemistry and Physics Discussions

Aerosols can travel long distances which increase the time they are exposed to radiation and the probability of interaction with clouds. In addition, the accumulation mode (0.1 μm < particle size < 2.5 μm) interacts most effectively with solar radiation, although the nuclei-mode aerosols (0.1 μm < particle size) are mostly found over the continents and coastal areas, directly related to human activities. Nuclei-mode aerosols account for about 10% of the aerosols of the globe (Textor et al., 2006). Aerosols emitted by natural sources are the dominant type in the climate system. In climate models, aerosols are generally divided into five general categories: dust, marine spray, sulphur aerosols or sulphate, and carbon compounds, which are divided into two subcategories: particulate organic material and Black Carbon (Chin et al., 2002).

The direct radiative effect of aerosols can absorb and scatter radiation in the shortwave band and longwave band, which directly impacts the radiative balance of the climate system (Forster et al., 2007). The net impact of the direct radiative effect of aerosols decreases the available solar energy at the surface. In the last decades, there has been a 2.7% reduction observed on the incident direct solar irradiance at the surface, a phenomenon known as 'Global Dimming' (Stanhill and Cohen, 2001). Although the mechanisms associated with the direct radiative effect of aerosols are well described in the literature, uncertainties are still significant, especially with respect to the special and temporal distribution of the aerosols in the atmosphere (Forster et al., 2007; Fletcher et al., 2018). In addition, the radiative effects of aerosols can impact different compartments of the climate system, such as the biosphere, for example.

The biosphere interacts with the climate system through biogeophysical and biogeochemical processes, which can cause both, positive and negative responses on the radiative balance, and some of these responses, especially at a local scale, can be quite significant (Wang et al., 2014; He et al., 2017; Persad and Caldeira, 2018).

The overall reduction of incident radiation at the surface has negatively impacted gross primary productivity (GPP) in light limited ecosystems (Black et al., 2006; Unger et al., 2017; Ezhova et al., 2018). In addition, a decrease in total solar radiation is followed by an increase in its diffuse component, which in turn can increase plant productivity due to a higher production efficiency per unit of incident radiation in the canopy, an effect known as 'the diffuse fertilization effect' (Kanniah et al., 2012). In ecosystems with densely vegetated canopies, the direct shortwave radiation reaches the upper part of the vegetation canopy, while most leaves at medium canopy height or at bottom canopy layers remain shaded. Carbon assimilation increases under atmospheric conditions with moderate aerosol load and high fraction of diffuse radiation (Niyogi et al., 2004) and decreases as the concentration of aerosols increases to a level where the overall radiation is substantially reduced (Yamasoe et al., 2006).

https://doi.org/10.5194/acp-2019-167
Preprint. Discussion started: 7 June 2019

Atmospheric Chemistry and Physics Discussions

The spatial distribution and nature of the shortwave radiation is critical for the productivity of terrestrial ecosystems and further studies on the impacts of light limitation on vegetation productivity are needed. In light limited ecosystems such as rainforests and temperate forests, the radiative impact of aerosols on vegetation productivity must be evaluated in combination with other environmental factors, such as temperature and water (O'Sullivan et al., 2016.). With fieldwork and numerical studies in the Australian savannah, Whitley et al. (2011) suggested that vegetation productivity was more influenced by light limitation than by water limitation. Actually, the response of photosynthetic capacity to an increase in the concentration of atmospheric aerosol has been extensively studied over almost the past two decades (Roderick et al., 2001; Niyogi et al., 2004; Yamasoe et al., 2006; Oliveira et al., 2007; Mercado et al., 2009; Doughty et al., 2010; Zhang et al., 2010; Kanniah et al., 2012; Tang and Dubayah, 2017) through observations (Steiner et al., 2013) and modeling (Moreira et al., 2017.) frameworks.

In this paper, however, we investigate the impact of atmospheric aerosols on the carbon balance over three sites in South America, in the deforestation arch of the Amazon forest, making use of a novel approach, combining two different types of modeling techniques. First, we make use of Artificial Neural Networks (ANNs) to build a new modeling framework from scratch relating a number of state variables (radiation, temperature, humidity, as well as the aerosol optical depth) with energy and mass fluxes for three study sites representing a range of structurally different ecosystems in the Amazon; and second, a radiative transfer scheme driven with a unique aerosol optical model developed in Rosário et al. (2009) and described Rosário et al. (2011). A recent study has performed a modeling evaluation of the radiative impact of aerosols over a temperate forest with complex structure in the USA (Lee et al., 2018.), but the studies in the Amazon remain mostly observational.

The main goal of this paper is to investigate, step-by-step, the effects of the atmospheric aerosol on the variability of CO_2, sensible (H), and latent (LE) heat fluxes in the Amazon region over the deforestation arch, based on the study of three specific experimental sites. The use of ANNs allows to build up a statistical modeling framework relating meteorological (i.e., temperature, humidity, friction velocity) and radiative variables (i.e., incident photosynthetically active radiation (PAR) incident at the top of the canopy, the percentage of diffuse PAR) to mass and energy fluxes in the forest in a first approach to address the radiative impacts on mass and energy fluxes. The follow up analysis is based on the derivation of a second group of ANNs relating radiative variables with meteorological ones in order to identify the second order effect of aerosols on surface fluxes. Finally, we make use of the radiative transfer (RT) theory with a process-based RT model to create a hypothetical scenario without aerosols and estimate the potential fluxes of mass and energy, not only considering the first order impact of aerosols, but also the second order impact by making use of two distinct groups of ANNs.

https://doi.org/10.5194/acp-2019-167
Preprint. Discussion started: 7 June 2019

Atmospheric Chemistry and Physics Discussions

With this approach, this study evaluates: (i) the impacts of aerosol optical depth at 550 nm on fluxes of heat, water, and CO_2; (ii) the characteristics of aerosol present in each of the experimental sites; and (iii) the isolated impact of aerosols on mass and energy fluxes through statistical modeling with ANNs, in comparison to other environmental factors, such as temperature, moisture, and turbulence.

2 Materials and methods

2.1 Sites

The deforestation arch consists of 248 municipalities in Brazil going from the state of Rondônia to the state of Maranhão, across the Brazilian savannah and Amazonian biomes (Araújo Junior et al, 2001), about 3,000 kilometres long and up to 600 kilometres wide. Between July and October 1987, the region of the deforestation arch lost approximately 50,000 km of forests in the states of Pará, Mato Grosso, Rondônia, and Acre, and released more than 500 million tons of carbon into the atmosphere, in which 44 million tons in the form of CO_2 (Song et al., 2015). The three flux sites evaluated in this paper are in the Brazilian deforestation arch (**Fig. 1**).

2.1.1 Bananal Island

The Bananal Island is the largest island in a river on the planet, with approximately 2 million hectares and almost 360 km in the North-South direction and 80 km in the East-West. The Bananal Island is a floodplain region. The flux tower of Bananal Island was installed in the Northern part of the island, in the limits with the Canton State Park, by the Laboratory of Climate and Biosphere of the Institute of Astronomy, Geophysics, and Atmospheric Sciences of the University of Sao Paulo. The average height of the canopy is approximately between 15 to 18 m. The instrumental platform was mounted in a 40 m high structure located approximately 2 km east of the Araguaia River, at the geographic coordinates 9° 49.27' S; 50° 08.92' W, at 120 m a.s.l. The data monitoring started on the 27th October 2003 and the project was based on the facilities of the Canguçú Research Centre of the Instituto Ecológica - UFT, approximately 20 km south of the micrometeorological tower (Borma et al., 2009).

2.1.2 Rebio Jaru

In the north-eastern part of the state of Rondônia, Brazil, the Jaru Biological Reserve has approximately 60,000 ha. The entire basin of the Tarumã river is in the reserve and covers about 75% of the unit. The land has a large number of small streams and springs keeping a moist vegetation throughout the year. The vegetation is mainly characterized as an Open Tropical Forest with some palm trees. There are also few areas with lianas and bamboo trees, as well as small spots of dense ombrophiles forest, characteristic of the Amazon region (IBAMA, 2006). The average height of the canopy is approximately 35m, but some trees can reach up to 45m. The tower is located

https://doi.org/10.5194/acp-2019-167
Preprint. Discussion started: 7 June 2019

Atmospheric Chemistry and Physics Discussions

1,240 m from the river bank in a more preserved region (Gomes, 2011). Data from the Rebio Jaru were collected from August to October 2007, at the geographic coordinate 10° 04.71' S; 61° 56.01' W 148 m a.s.l. Eddy-covariance instruments were installed in the 62 m height (Bosveld and Beljaars, 2001).

2.1.3 Sinop

This study site is located in an area of logging with forest management in Fazenda Maracaí. The farm is located to the northwest, approximately 50 km, from the centre of Sinop, Mato Grosso, Brazil, at coordinates 11° 24.70' S; 55° 19.39'W, at 423 m a.s.l. The Maracaí farm consists of a transitional tropical forest (between Brazilian savannah and open ombrophiles forest) with a continuous canopy, composed of trees from 25 to 28m in height (Vourlitis et al., 2008). The vegetation consists of perennial trees that is characteristic of the transition forest in Mato Grosso. The diversity is high, and there is no predominance of a single tree species. There are approximately 80 species and 35 families of trees with diameter at breast height around 10 cm. The climatological seasonality for the ecotone of the transition forest is similar to that of the tropical and closed forest. The sonic anemometer was installed at 42 meters height. The site is part of the LBA's integrated project and has been carrying out measurements of this nature since 1999.

2.2 Flux tower data

Surface fluxes of CO_2, sensible heat, and latent heat were obtained through the eddy covariance technique applied to data collected with sonic anemometers and infrared gas analyzers installed in flux towers located at Bananal Island, Sinop, and the Jaru Biological Reserve (Rebio Jaru). Fluxes were obtained with temporal resolution of 30 minutes. Measurements of meteorological variables, such as temperature, relative humidity, and wind speed were collected. Except for the tower in Sinop, the other towers presented radiative measurements such as incident solar radiation and, incident and reflected PAR. For Sinop, these variables were calculated by a radiative transfer model, libRadtran, further described in Section 3.1.

Geographic coordinates, altitudes, flux tower heights, and the type of sensors used in each one of the three sites are presented in **Table 1**. A Multifilter Rotating Shadowband Radiometer data provided aerosol optical depth at 550 nm estimates per minute and 30 minutes averaged values were calculated, available only for the Rebio Jaru site.

The study period of this work was limited to the dry season, since **(a)** the maximum numbers of fire outbreaks occur in August, September, and October. **(b)** In terms of the temporal distribution of the aerosol optical depth, there is a significant increase in the months of August, September, and October. And, **(c)** the analysis of the

https://doi.org/10.5194/acp-2019-167
Preprint. Discussion started: 7 June 2019


Atmospheric Chemistry and Physics Discussions

intrinsic properties of the aerosols becomes important because it has indications of its chemical composition and size of the particles. Only the months of August, September, and October were considered in this analysis in order to keep consistency of the type of aerosols being evaluated.

2.3 MODIS data

The aerosol optical depth (AOD) at 550 nm used in this study was obtained from the Moderate Resolution Imaging Spectroradiometer (MODIS) for Bananal Island and Sinop. Except for Rebio Jaru, where AOD values were obtained in situ with shadow band radiometer (MFRSR) (**Table 1**). MODIS is an instrument on board of the Terra and Aqua satellites. The Terra's orbit around the globe is synchronized and flies from north to south across the equator line in the morning (~ 10:30 local time), while the Aqua presents passages from south to north by the equator in the afternoon (~ 13:30 local time). MODIS observes the entire ocean surface of the Earth and almost the entire terrestrial surface in a period of 1 to 2 days and acquires data in 36 spectral bands. The aerosol product from MODIS is a measured of the aerosol optical depth over the oceans and a portion of the continents, globally. In addition, the aerosol size distribution is derived over the oceans, and the aerosol type over continents. Daily Level 2 data is produced with a spatial resolution of 10 x 10 km^2 over nadir. Two groups of MODIS aerosol data products were collected: MOD04_L2, containing the data collected from the Terra platform, and MYD04_L2, containing the data collected from the Aqua platform. The MODIS aerosol product is used to build the climatological variance of aerosols, sources and sinks of specific types of aerosols (e.g., sulphate aerosols, biomass burning), the interaction of aerosols with clouds, and atmospheric corrections of surface reflectance obtained from remote sensing.

Pre-assumptions about the general structure of aerosol size distribution are necessary for the inversion of the MODIS data and the distribution is described as two log-normal curves: a unique mode, to characterize the particles of accumulation mode (aerosol radius < 0.5 μm) and a single coarse mode to describe dust and salt particles (aerosol radius > 1.0 μm). The aerosol parameters that are thus recovered are: the relationship between the two modes (fine and coarse), spectral optical depth, and mean particle size. The quality control of these products is based on the comparison with terrestrial stations and climatology. We used instantaneous and monthly fields of the aerosol optical depth at 550 nm (AOD550nm), referring to collection 051 (Hubanks, 2012), level 2. The pixels over the flux towers were considered. Episodes contaminated by clouds were excluded from the analysis.

The MODIS aerosol data was acquired at the moment of each satellite overpass (Terra and Aqua) over the site of interest, and a single point was used to represent the 30 minutes interval. Uncertainties associated with each

https://doi.org/10.5194/acp-2019-167
Preprint. Discussion started: 7 June 2019

Atmospheric Chemistry and Physics Discussions

variable were estimated from the standard deviations obtained for the 30-minute intervals, except for the MODIS AOD550nm measurements, in which the uncertainty of the AOD550nm in an area of 10 x 10 km was estimated following Levy et al. (2009) as,

$$\sigma_\tau = \pm(0.05 \pm 0.15\tau) \quad (1)$$

In Rebio Jaru, in situ AOD measuring was conducted in a relatively limited period of time, covering only part of the dry season of 2007, yet the high temporal resolution of the aerosol optical depth data (every minute) enabled a more robust analysis of the diurnal cycle. On the other hand, in Bananal Island and in Sinop, the time series of flux measurement was longer (from 2003 to 2008, and from 2005 to 2008, respectively). However, AOD data was limited to maximum two points a day from MODIS, but the analysis of these experimental sites presented possibilities of characterization of the interannual cycles.

3 Models

3.1 libRadtran

The radiative transfer model libRadtran1.6-beta (Mayer and Kylling, 2005) was used to perform calculations with the incident solar radiation at the Top of the Atmosphere (TOA) specified for the Amazon region with a tropical atmosphere profile. Ozone concentrations were set to 300 DU based on values obtained by Rosário et al. (2009), who found an average value of integrated ozone content in the atmospheric column of 257 DU. In this paper, surface albedos from the International Geosphere-Biosphere Programme (IGBP) classification (Loveland and Belward, 1997) were used.

For the three sites, the surface type was set to a deciduous broadleaf forest. The day of the year provides information about the Earth-Sun distance, which affects the amount of radiation incident at the TOA, and it was also used as input to the code. The correction for molecular absorption, parameterized from the LOWTRAN model (Pierluissi and Peng, 1985), as well as adopted by the SBDART code (Ricchiazzi et al. 1998) was implemented. The resolution of the corrections for molecular absorption was 0.5 nm at wavelengths below 350 nm and 1.0 nm above. The DISORT method (DIScrete ORdinate Radiative Transfer Solvers) was used to solve the radiative transfer equations because of its versatility and broad use (Mayer et al., 2010). Four streams were used in the simulations performed in this paper. Previous studies have shown that differences in incident irradiance at the surface with at least 4 streams are minimal (Mayer et al., 2011). PAR waveband ranges between 400 and 700 nm and total solar radiation between 280 and 4000 nm.

https://doi.org/10.5194/acp-2019-167
Preprint. Discussion started: 7 June 2019

Atmospheric Chemistry and Physics Discussions

The input data required to describe the intensive optical properties of the aerosols were obtained from models created with the Mie theory from Rosário (2011), derived from the Aerosol Robotic Network (AERONET) products for three experimental sites: Alta Floresta, Abracos Hill, and Rio Branco. These models carry spectral information about the linear extinction coefficient (Q) in km^{-1}, the single scattering albedo (ω_0), calculated from the Henyey- Greenstein method (Henyey and Greenstein, 1941). Spectral resolution of the aerosol model in the PAR spectral region was 25 nm, and over the entire solar spectrum it varied from approximately 10 nm at shorter wavelengths up to 700 nm at longer wavelengths.

Three optical models were developed for the biomass burning aerosol emitted over Amazon, which are different in scattering and absorption properties: a more scattering, an intermediate type, and a more absorbing aerosol type. Also, in this study, sensitivity analysis performed with data from the Biological Reserve of Jaru showed that the more scattering aerosol model is the one that best represented the biomass burning aerosols of that season, associated to higher values of AOD550nm. Therefore, in this study, the aerosol model used for all three study sites was the more scattering type.

The specific input parameters of the radiative transfer equations are: solar zenith angle and the aerosol optical depth at 550 nm. The model provides the integrated value of the downward direct irradiance, the downward diffuse irradiance, and the upward diffuse irradiance, at the altitude determined by the user. All calculations were determined at the surface. From these values, it is possible to obtain the descending global irradiance (the sum of the contributions of the direct and diffuse irradiance incident at the surface) and the diffuse fraction, i.e., the ratio between the diffuse and incident global irradiance at the surface.

3.2 Artificial Neural Networks

Artificial Neural Networks (ANNs) have great potential because of their capacity to represent the complexity of the phenomena that are analyzed through them. Traditionally, simulation systems, whether physical or statistical, have great difficulty in reproducing complex responses of natural events. ANNs can be considered a network of many relatively simple processors, called units or nodes, in which there is a small amount of local memory. In ANNs, these basic local memory units are commonly layered and communicate through channels or connections, and operate only on their own media, that is, with their local data and their input parameters (Papale and Valentini, 2003). They can be seen as robust parallel processor with natural ability to store knowledge gained from experimentation and make this learning available for future use. This means that, from this method, it is possible to create hypothetical scenarios to evaluate the behavior of the output variables, in relation to possible modifications in the input variables.

https://doi.org/10.5194/acp-2019-167
Preprint. Discussion started: 7 June 2019

Atmospheric Chemistry and Physics Discussions

ANNs are trained from examples contained in the total set of input data. The "weights" are randomly provided at the beginning of the process and modified according to the rule used in the backpropagation method. In this paper, two methods of resolution of ANNs were used: i) the Multilayer Perceptron (MLP) is a direct and unidirectional power supply model of artificial neural networks, which maps the input data sets to an appropriate set of output data. The MLP uses the backpropagation technique to train the networks. The most commonly used functions in this method are both sigmoid (Bayram et al., 2016); and ii) the Radial Basis Function (RBF) uses functions of radial basis as a function of activation of the nodes of the neural networks. The RBF method typically has three layers: the input, the intermediate, with a non-linear activation function and the output with a linear function. The input parameters are modeled as a vector composed of real numbers, and the outputs are scalar functions with vector input values (Bayram et al., 2016).

For all ANNs used in this paper, 200 neural networks were generated for each one of the different output variables, from all three study sites, and only the one with the smallest error between modelled and observed output was evaluated. From the total dataset, 70% of the data were randomly chosen and used in the training process of the ANNs, 15% in the validation process, and 15% in the testing process. The set used in the training process has the function of exemplifying relations between inputs and outputs to the ANN.

The variables used to train the ANNs were: incident photosynthetically active radiation incident at the top of the canopy (PAR_i) in Wm^{-2}, the partitioning of photosynthetically active radiation in its diffuse form (PAR*dif*) in percentage, derived from the method of Reindl et al. (1990), the solar zenith angle (SZA) in degrees, the average air temperature in the canopy (T) in degrees Celsius, the vapor pressure deficit (VPD) in kPa, the friction velocity (u^*) in ms^{-1}, and the aerosol optical depth at 550 nm (AOD550nm). Therefore, seven variables were used as inputs of the ANN and the flux of carbon dioxide (FCO_2), in μmol CO^2 $m^{-2}s^{-1}$, was selected as output.

The best carbon flux ANN for all sites presented similarities such as: all three were generated from the RBF training model, used a Gaussian function for the activation of the hidden units, and the identity function for the activation of the output. However, the ANNs presented different number of hidden units. The network generated for the Bananal Island presented 30 hidden units, the one generated for Sinop used 21, and for Jaru, 19. Basically, the larger the number of hidden units in a neural network, the more robust the model is, i.e., the neural network has a greater capacity to model more complex relationships. At the end, the number of hidden units provides an indication that the database of the three analyzed sites presented different complexities in the relationship between the variables introduced at the moment of the construction of the networks. However, the functions that best managed to describe these relations were the same and the difference between them is the error magnitude between output data used for training and the model output.

https://doi.org/10.5194/acp-2019-167
Preprint. Discussion started: 7 June 2019

Atmospheric Chemistry and Physics Discussions

The performance of the ANN results was evaluated using the Pearson coefficient (r), RMSE and MAE, defined as:

$$r = \frac{\sum_p (y - \text{mean}(y))(t - \text{mean}(t))}{\sqrt{\sum_p (y - \text{mean}(y))^2 (t - \text{mean}(t))^2}} \quad (2)$$

Where p is the total number of examples, y are the calculated values, and t are the observed values.

Root Mean Square Error (RMSE) is used to evaluate differences between the values predicted by a mathematical or physical model (y) and the observed values (t). RMSE is a good measure of the accuracy of a model, but only to compare calculations and observations of the same variable, since it is scale dependent. It is obtained by the following equation:

$$RMSE = \sqrt{\frac{\sum_p (y - t)^2}{p}} \quad (3)$$

Finally, the use of the Mean Absolute Error (MAE) does not take into account if an error was overestimated or underestimated, once it is characterized as the average of the errors committed by a model and can be obtained from the following equation,

$$MAE = \frac{1}{p} \sum_p |y - t| \quad (4)$$

4. Results

4.1 Evaluation of ANNs for CO_2, sensible heat, and latent heat fluxes

In the absence of clouds, aerosols were responsible for changing the amount of solar radiation available at the surface and the partition between direct and diffuse radiation. This, in turn, impacted surface temperature, water vapor, among other changes able to affect photosynthesis.

Flux data was combined with meteorological and satellite data. It is important to emphasize that the flux data have a sample interval of 30 minutes, while the satellite data is a 'snapshot' of the atmosphere when the passage occurs in a very short time interval, which registers a value referred to a single minute, but over a 10 x 10 km^2 area.

From the integration of the database it was possible to make an analysis using ANNs. Some precautions were taken in order to avoid misleading analysis of the ANNs. For example, values of u^* smaller or equal to 0.2 $m.s^{-1}$ were excluded from the training, testing, and validation processes to avoid uncertain CO_2 flux data collected in episodes with less turbulence, and therefore, a less mixed atmosphere. All data points for all variables above or below three standard deviations were excluded from the input datasets of the ANNs because they were considered to be outliers.

https://doi.org/10.5194/acp-2019-167
Preprint. Discussion started: 7 June 2019

Atmospheric Chemistry and Physics Discussions

Seven variables were used as inputs of the ANNs: photosynthetically active radiation incident on surface (PARi), in $W.m^{-2}$, the partition of photosynthetically active radiation in diffuse form (PARdif), in%, derived from the method of Reindl (1990), the solar zenith angle (SZA), in degrees, the mean air temperature in the canopy (T) in degrees Celsius, the vapor pressure deficit (VPD) in kPa, the friction velocity (u*), in ms^{-1} and the aerosol optical depth at 550 nm (AOD550nm). The flux of carbon dioxide (FCO_2) (in µmol CO2 $m^{-2}s^{-1}$) was selected as output.

Figure 2 shows the FCO_2 data set used for validation, obtained through the eddy covariance method, on the x-axis (Eddy), and the ones calculated by the generated ANN, on the y-axis, with the respective Pearson coefficient (r), RMSE, and MAE, for all three sites.

The Rebio Jaru site presented the highest Pearson coefficient (0.82) of the three evaluated sites, which represents a high correlation between the measured and modelled CO_2 flux data. This site presented continuous AOD550nm data coverage throughout the day. At the other two sites, a single day had a maximum of two AOD550nm data points associated with the passages of the Terra and Aqua satellites. This result indicates that a continuous daytime coverage of AOD generated a more robust ANN influencing FCO_2 with more predictability.

Figure 3 shows examples of the diurnal variation of FCO_2 compared to the values simulated by its respective ANN, for the Rebio Jaru site. It is possible to notice that on all evaluated days, the ANN results followed the measured data. During the evaluated period (August, September, and October 2007), the mean value of FCO_2 was -12.2 µmol CO_2 $m^{-2}s^{-1}$, while the average FCO_2 generated by the ANN for the same period was -12.4 µmol CO_2 $m^{-2}s^{-1}$, a relative difference of 1.9%.

The Bananal Island site presented the lowest values of RMSE (3.20) and MAE (2.43). because of its long temporal series, from October 2003 to December 2008, with 320 input points, which was important to establish a more robust mapping of the intra-seasonal variability. Throughout the evaluated period, the mean observed FCO_2 for Bananal Island was -7.0 µmol CO_2 $m^{-2}s^{-1}$, while the average FCO_2 generated by the ANN was -7.1 µmol CO_2 $m^{-2}s^{-1}$, a relative difference of 1.3%.

The Sinop site presented the largest discrepancies between the model and observed FCO_2 with a Pearson coefficient of 0.58, RMSE of 5.69 µmol CO_2 $m^{-2}s^{-1}$, and MAE 4.78 µmol CO_2 $m^{-2}s^{-1}$. A database of intermediate size compared to the other sites (237 points), no PAR measurements were performed at Sinop, but values were generated with the radiative transfer model libRadtran. The errors associated with the outputs of the radiative transfer model were included in the neural network training process. The relative difference between the mean observed and simulated FCO_2 was 1.2%.

In order to evaluate the radiative effects of aerosol optical depth on turbulent energy fluxes, the same type of analysis performed for carbon dioxide flux, was done for sensible heat flux (H) and latent heat flux (LE). The

https://doi.org/10.5194/acp-2019-167
Preprint. Discussion started: 7 June 2019

Atmospheric Chemistry and Physics Discussions

evaluated period was also the same, August, September, and October, the dry and burning season in the region. For all three experimental sites the ANNs were made from the same variables used in the networks related to FCO_2.

All data points above or below three standard deviations were excluded from the input sets, because they were considered to be outliers and the choice of ANNs.

As for FCO_2, Rebio Jaru presented the highest Pearson coefficient (0.93) for sensible heat flux results. However, the same behavior was not observed when evaluating latent heat flux, which presented a relatively low Pearson coefficient (0.25) in comparison. In general, the overall results of LE compared to H presented relatively smaller values of Pearson coefficients. The diurnal cycle of H is more well-behaved in relation to LE as it depends on the diurnal cycle of temperature. Latent heat flux, on the other hand, is greatly influenced by advection of moisture coming from other sources not exclusively related to stomatal opening by the local vegetation. The presence of springs nearby could explain peaks on local maxima of latent heat flux.

This can be seen in **Figure 3**, which shows the diurnal cycle (for some days of the experiment) of measured H and LE fluxes (black dots) and the respective curves calculated from ANNs (red lines). During the evaluated period (August, September, and October 2007), the mean H observed was 117.4 Wm^{-2}, while the average of H generated by ANN for the same period was 111.7 Wm^{-2}, a relative difference of 4.9%. For LE, the mean value of the observed data was 218.1 Wm^{-2} and the average value generated by ANN was 218.7 Wm^{-2}, a relative difference of 0.3%. Although the analyzes performed between the validation data and those obtained through ANNs presented better results for H, the relative difference between the mean values of LE - calculated and observed - was lower.

It is important to emphasize that the analysis performed between the validation data and the modelled data generated by ANNs is a way to determine if the neural network is robust. This does not mean that a low Pearson coefficient indicates that a given ANN has low predictability. The evaluation of the relative deviation is a way of measuring the accuracy of an ANN. Although it is possible to note in **Figure 2.b** that the ANN of H could better approximate the measured values, the relative error associated with ANN of LE was around 4.6% lower.

Bananal Island presented intermediate values for Pearson's coefficient (0.65 for H and 0.59 for LE), which indicates an average correlation between the observed and the modelled data. For relative deviations, the values were lower than 3% for H data and lower than 1% for LE.

For Sinop, the analyzes of H presented a Pearson coefficient of 0.73, considered from medium to high performance of the ANN, and a relative deviation of 0.5%. For LE, the Pearson coefficient was 0.52 and the relative error was 1.2%.

https://doi.org/10.5194/acp-2019-167
Preprint. Discussion started: 7 June 2019

Atmospheric Chemistry and Physics Discussions

4.2 Modeling CO_2 fluxes with ANNs with constant temperature and moisture

From the generated ANNs, tests were performed to determine the behavior of FCO_2 in different scenarios for all three evaluated sites. In the first test, the values of T, VPD, and u* were fixed in order to isolate aerosol radiative effect on the availability of photosynthetically active radiation at the surface and the partitioning of it in its direct and diffuse forms. This first test is hypothetical, since it is known that the fixed variables also suffer influences of AOD550nm. In the test, AOD550nm varied from 0.0 to 2.0 and the radiative transfer model libRadtran was used to estimate values of PAR_i and PAR_{dif} values, for three different solar zenith angles (15º, 30º, and 45º). The results related to Bananal Island can be seen in **Figure 4**. The other sites showed similar behavior.

The values of T, VPD, and u* were fixed at the 'optimal point' of FCO_2, i.e., for which values of T, VPD, and u*, FCO_2 presented the largest absolute values. For the other sites, arbitrary values were fixed, close to those found at the Bananal Island. **Table 2** shows the values of T, VPD, and u* fixed for each one of the evaluated sites. **Figure 5** shows the variation of FCO_2 in relation to AOD550nm for three different SZAs (15º, 30º, and 45º), in the three evaluated sites. For Bananal Island and Rebio Jaru, the increase in AOD550nm generates an initial decrease in the absolute values of FCO_2, for almost all SZAs, except for the solar zenith angle of 30º in Bananal Island, which appears to have no impact on CO_2 flux until AOD550nm ~ 0.25. However, from this value on, the FCO_2 values show a decreasing trend.

The FCO_2 in Bananal Island presents a minimum point with the variation of AOD550nm, while in Rebio Jaru, FCO_2 presents a more stable behaviour. In the Bananal Island, after the minimum point of the curve, FCO_2 starts to increase with AOD550nm, i.e., there is an optimal range of AOD550nm, which is dependent on the SZA. For SZA = 15°, this interval is associated with AOD550nm between 0.59 and 0.93. For SZA = 30°, the interval is narrower, with AOD550nm ranging from 0.57 to 0.61. And for SZA = 45 °, AOD550nm is between 0.45 and 0.55. For higher values of AOD550nm (above 1.75), the behavior of FCO_2 also stabilizes, but at different points, dependent on SZA.

In Rebio Jaru, on the other hand, this behavior associated to an 'optimal range' of AOD550nm influence on the FCO_2 curve is not observed. It is possible to identify a value of AOD550nm where the value of FCO_2 stabilizes and does not present significant variations anymore. This value of AOD550nm, associated to the stabilization of the curves, also appears correlated with the solar zenith angle. For SZA = 15°, this value of AOD550nm is 0.98, for SZA = 30° is 0.88 and for SZA = 45° is 0.65. When analyzing the results for Sinop, this behavior of decrease in the absolute value of FCO_2 with the increase of AOD550nm is not verified. The addition of AOD550nm values from 0.0 to 2.0 generates increases in absolute values, that is, the CO_2 changes between the local vegetation and

https://doi.org/10.5194/acp-2019-167
Preprint. Discussion started: 7 June 2019

Atmospheric Chemistry and Physics Discussions

the atmosphere decrease with higher aerosol load. This behavior is observed up to a value of AOD550nm from where FCO_2 value stabilizes, depending on the SZA. For SZA = 15°, this value of AOD550nm is 1.85, for SZA = 30° is 1.70, and for SZA = 45° AOD550nm = 1.25.

4.3 Modeling temperature, humidity, and wind with ANNs

In the first test, temperature, VPD, and u* were fixed as described in **Table 2**, but, these variables are directly related to the available energy at the surface and, therefore, these variables would also be impacted in the presence of aerosols. Artificial neural networks were built from the same database used to make the previous ANNs but varying its input and output values.

The first variable to be evaluated was the temperature. Three variables were used as input parameters in the training processes of the temperature ANN: PAR_i (Wm^{-2}), PAR_{dif} (%) and SZA (º). These variables were chosen as inputs for the neural network of temperature because radiation directly impact surface temperature. The available energy at the surface is proportional to PAR_i and PAR_{dif}, linked to the diurnal cycle.

The second evaluated variable was VPD. This variable is related to temperature, which is related to PAR_i, PAR_{dif}, and SZA. Thus, these 4 variables were used as inputs values in the construction of the VPD ANN.

Finally, u* is also affected by energy available at the surface but in a lower degree once it is directly dependent on wind speed. All other variables (except for the AOD550nm itself, in order to avoid overtraining) were used as input values in the construction of the u* ANN.

Figure 6 shows data used for the validation, i.e., without interference in the construction of the networks. The values of the x-axis correspond to the observed values, and those of the y-axis, to the values generated by the neural networks. The results for the neural networks of VPD, for all evaluated sites, were the most compatible with the values observed and they presented a Pearson coefficient greater than 0.9. This is mainly because VPD is closely related to temperature. The explanation of the variance of VPD through the variables used as inputs of the ANNs was mainly governed by temperature. In Bananal Island, temperature explained 50.5% of the VPD variance, in Rebio Jaru and Sinop, 65.6% and 38.1%, respectively. Temperature and friction velocity presented a moderate Pearson correlation (between 0.3 and 0.7) for all cases. However, in the overall sensitivity analysis, PAR_i was mostly responsible for the explanation of the variance of temperature.

https://doi.org/10.5194/acp-2019-167
Preprint. Discussion started: 7 June 2019

Atmospheric Chemistry and Physics Discussions

4.4 Isolating the radiative impact of aerosols on CO_2, sensible heat, and latent heat fluxes with ANN modeling

From the generated ANNs, a study performed in order to identify what the relative differences would be in FCO_2, H, and LE fluxes between real observed conditions and an atmosphere without aerosols, i.e., with AOD550nm = 0.0 for the evaluated cases.

First, the radiative transfer model, libRadtran, was used to obtain PAR_i and PAR_{dif} values for an atmosphere with AOD550nm = 0.0. For the calculations, the real values of SZA and day of the year were used. The results for the Rebio Jaru site can be visualized in **Figure 7**. For the other study sites, the same behavior of the curves is observed. It is possible to identify that the observed values of PAR_i are systematically lower than those obtained by the radiative transfer model, while the opposite is observed for PAR_{dif}. Aerosol decreases the incident shortwave global radiation at the surface by absorption and scattering processes, while it increases the percentage of diffuse radiation due to the scattering. From PAR_i and PAR_{dif} calculated for an aerosol-free atmosphere, temperature, VPD, and u* were calculated through the ANNs. The SZA values used as input in the libRadtran were the same as those used in the ANNs.

All variables obtained by both models (libRadtran and ANNs) - except for the values of AOD550nm, which were set at zero, and SZAs, which were kept the same as the original database - were used in calculations of fluxes of CO_2, H, and LE. **Table 3** summarizes the results. The mean real values and standard deviations of each of the variables of the initial set of data, the mean model values and the respective standard deviations are shown also for all variables. The relative difference between the means of the actual values and the simulated ones, indicating whether the model presented values larger than the real ones (positive), or smaller (negative).

PAR_i and PAR_{dif} variables agreed over the three sites, when comparing the actual and simulated values. The average of the modelled PAR_i values, without aerosol, was 12.4% higher than the average of the real values for the Bananal Island site, 29.8% higher for the Rebio Jaru, and 26.3% % higher for Sinop. On the other hand, the average of the model values of PAR_{dif} was 35.9% lower than the average of the real values for Bananal Island, 52.0% lower for Rebio Jaru, and 38.0% lower for Sinop.

Temperature also showed agreement regarding the increase of the mean values modelled in relation to the mean real values. In Bananal Island, the increase was 11.3%, in Rebio Jaru was 7.4%, and in Sinop the relative difference was 1.7%. The relative difference between the actual and modelled mean values of VPD and u * did not show agreement for the three experimental sites. However, Bananal Island presented a significant increase in VPD (~50%) for an atmosphere with no aerosols.

https://doi.org/10.5194/acp-2019-167
Preprint. Discussion started: 7 June 2019

Atmospheric Chemistry and Physics Discussions

As demonstrated by Doughty et al. (2010) for a tropical forest, there is a decrease of approximately 13% in the FCO_2 for every 1ºC increase in temperature, when it is above 28ºC. Due to the high correlation between VPD and T, the results of the model without aerosols agree with the authors.

For FCO_2, Bananal Island and Rebio Jaru presented higher mean modelled values, i.e., a lower exchange of CO_2 with the atmosphere is expected under the effect of episodes without aerosols. Sinop presented the opposite effect. This is mainly due to the differences in structural local characteristics of each site. The response of photosynthetic capacity to an increase in diffuse radiation may vary between different ecosystems and seems to be related to the different properties of canopies (Zhang et al., 2010; Kanniah et al., 2012; Tang and Dubayah, 2017). Niyogi (2004) showed that carbon assimilation grows with an increase in aerosol concentration in the case of forests and cultivated areas and decreases over pastures.

The surrounding areas of the flux tower in Sinop show several regions of pasture, which later became soy or maize plantations. For this reason, the less complex canopy structures in the region (with lower vegetation and more homogeneity in the vertical and horizontal distribution) have opposite responses to that proposed by the "diffuse fertilization effect" theory. The complexity of the canopies in Bananal Island and Rebio Jaru confirms the effect.

The same type of test was performed in order to evaluate the relative differences in H and LE under conditions of an observed aerosol concentration and a simulated atmosphere without aerosols, with AOD550nm = 0.0. In this test, energy (H and LE) fluxes were obtained using variables calculated by the models (libRadtran and ANNs), except for the values of AOD550nm (0.0) and SZAs, which were obtained through the original data. **Table 3** shows the average real values and the standard deviations of the fluxes, H and LE, for the observed database, the average model values and the relative difference between the means of the real values and the simulated ones.

For all three sites, the values of sensible and latent heat fluxes calculated through the ANNs for a scenario without aerosols were higher than the mean observed values. It was observed that, for all experimental sites, an aerosol-free atmosphere was associated with higher PAR_i and lower PAR_{dif} values, which means that in an aerosol-free atmosphere, there are conditions for more available energy at the surface, which may explain the increase in the mean values of sensible and latent heat fluxes. The higher availability of surface radiative energy proved to be used for the increase in temperature. The analysis of energy fluxes indicates that in the presence of aerosols, there is a total reduction in both heat and water exchange between the surface and the atmosphere over the evaluated sites.

Over all experimental sites, sensible heat flux was shown to be more susceptible to changes in AOD550nm compared to latent heat flux. This fact is greatly observed in Bananal Island and Rebio Jaru, but less in Sinop. A possible explanation for this phenomenon can be obtained by evaluating the absorption spectrum of water. The

https://doi.org/10.5194/acp-2019-167
Preprint. Discussion started: 7 June 2019

Atmospheric Chemistry and Physics Discussions

spectral region most affected by the presence of biomass burning aerosols is the PAR and evaluations were limited to this spectrum only. This spectral region interacts very little with water. Another possible explanation is due to the temperature rise of the canopy itself. The vegetation responds to temperature increase with a stomatal closure, which decreases evapotranspiration. Aerosols are more efficient in affecting the exchange of heat between the atmosphere and the vegetation than the exchange of moisture between the two.

5. Conclusions

In this study, we evaluated the impact of AOD550 nm on land fluxes of CO_2, sensible heat, and latent heat for three study sites located in the deforestation arch region of the Brazilian Amazon using a combination of ANNs and radiative transfer modeling.

Aerosols were responsible for changing the amount of solar radiation available at the surface and the partition between direct and diffuse radiation. The radiative impact of aerosols caused variations in the temperature and humidity, as well as in FCO_2. For the impact of aerosol on the flux of CO_2, the modelled values with ANN for Rebio Jaru indicated a strong dependence with solar zenith angle. Temperature and VPD were important in explaining FCO_2 variance for all study sites.

For Bananal Island and Rebio Jaru, the increase of AOD550nm initially generates a decrease in the absolute values of FCO_2 to AOD550nm ~ 0.25. However, for higher values of AOD550nm, FCO_2 decreased, which indicates higher photosynthetic rates. In Sinop this behavior is not observed.

We developed a group of ANNs relating meteorological and radiative variables for three sites in the Amazon region (**Fig. 8**). For Bananal Island, the behavior of decreasing FCO_2 with the increase of AOD550nm remains. For Rebio Jaru, the FCO_2 decreases with AOD550nm up to approximately AOD550nm = 0.50 and shows the opposite behavior after that. For Sinop, the behavior between both scenarios remained basically the same.

In order to obtain the total radiative impact of aerosols on FCO_2, a third test consisted of a study to define the relative differences in FCO_2 between conditions in the presence of aerosol and without aerosols (AOD550nm = 0.0) in a combination of two distinct methodologies: ANNs and radiative transfer modeling. The average of the modelled PAR_i values without aerosol was higher than the average of the real values for all sites, while the average of modelled values of PAR_{dif} was lower, as expected. Temperature also increased in the modelled scenario without aerosols in relation to the one containing aerosols. The relative difference between the actual and modeled mean values of VPD and u* did not show agreement for the three experimental sites.

Bananal Island and Rebio Jaru presented higher values of modelled CO_2 flux in the scenario without aerosol, while Sinop presented the opposite result. This is due to the canopy properties of Sinop and surroundings

https://doi.org/10.5194/acp-2019-167
Preprint. Discussion started: 7 June 2019

Atmospheric Chemistry and Physics Discussions

presenting several crop fields. For this reason, the less complex canopy architecture in the region acted to decrease photosynthetic response of the vegetation to less total incident PAR and more radiation in its diffuse form. We conclude that in the absence of aerosols, CO_2 flux from the atmosphere to the surface in Rebio Jaru could be reduced to more than half as its current values in the presence of aerosols. This effect is only observable by taking secondary effects into account.

The same type of evaluation was performed for the fluxes of sensible heat and latent heat using ANNs. When evaluating the variables that best explain the variance of sensible heat flux for Bananal Island, VPD and T showed a strong influence of 27.4% and 23.7%, respectively. This fact indicates that energy fluxes of Bananal Island are influenced by temperature. In the case of Rebio Jaru, PAR_i explained about 17% of the variance of H. For Sinop, there is no favorable variable explaining the variances of H and LE. However, the friction velocity (u*) presented the highest index of sensitivity (15%), which indicates that the variance of both energy fluxes was more influenced by turbulence itself.

In the first test, the behavior of the fluxes with AOD550nm showed quite similarities in all three sites. The average behavior of both, H and LE, was decreasing by an increasing aerosol optical depth. The increase in aerosol concentration decreases total incident radiative energy at the surface and, thus generates a systematic decrease in H and LE. In the second test, the variation of other meteorological variables affected the fluxes and, although differences were present, the general behavior of energy fluxes with aerosol optical depth remained. Sensible heat flux and latent heat flux decreased with higher AOD550nm. In the scenario with AOD550nm = 0.0, the values of sensible and latent heat fluxes were higher than the observed values. This indicates that in an atmosphere without aerosols, more energy is available at the surface. Sensible heat flux was shown to be more susceptible to changes in AOD550nm compared to latent heat flux. This fact is reported in the Bananal Island and Rebio Jaru data sets, but less in Sinop. The radiative spectral region most affected by the presence of the biomass burning aerosols is the PAR, and only the aerosol optical depth at 550 nm was evaluated. The radiation at 550 nm interacts little with water vapor. Also, an increase in canopy temperature may lead to stomatal closure decreasing total evapotranspiration, which can impact latent heat flux negatively.

The two group of ANNs developed in this study, i.e., characterizing the first and second order radiative impact of aerosols on mass and energy fluxes, can be used for flux data gap-filling, as well as modeling and evaluating future climate. More evaluations of the impact of aerosols on energy fluxes throughout the Amazon basin are needed, and machine learning techniques are an efficient and accessible tool to develop these studies. Coupling machine learning techniques at local and regional levels with land surface models (Moreira et al., 2017) and climate models (Malavelle et al., 2019).

https://doi.org/10.5194/acp-2019-167
Preprint. Discussion started: 7 June 2019

Atmospheric Chemistry and Physics Discussions

Data availability

Flux and aerosol data used in this study are available in https://doi.org/10.6084/m9.figshare.8239691.v1 under license Apache2.0.

Author Contributions

R.K.B. designed the study, conducted the analysis, and wrote the manuscript. M.A.Y. coordinated the intensive field campaign at Rebio Jaru in the dry season of 2007 and contributed to the writing of the manuscript. N.M.E.R. developed the aerosols optical models. H.R.R., J.S.N., and A.C.A. coordinated the measurements and shared the flux data for Bananal Island, Sinop, and Rebio Jaru, respectively.

Competing interests

The authors declare that they have no conflict of interest.

Acknowledgments

This work was conducted during a MSc scholarship financed in part in part by the Coordenação de Aperfeiçoamento de Pessoal de Nível Superior - Brasil (CAPES) - Finance Code 001, at the University of Sao Paulo, Brazil. M.A.Y. acknowledges FAPESP (grant number 06-56550-5) for funding the intensive campaign at Rebio Jaru. The authors would like to thank the staff from ICMBio at Rebio Jaru. Dr. Renata Aguiar, Federal University of Rondônia, Campus Ji Paraná, and the LBA local office for collecting and processing the flux data. Also, thanks to Mr. Frederico and students of the LBA local office, as well as to Mrs. Ruth Souza and other employees for the support during the field campaign.

References

Araújo Junior, G. J. L. D. de, Pereira, J. A. R., Silva, T. M. V. da, Mafra, H., Brass, J. A., Lockwood, R. N., Higgins, R. G. and Riggan, P. J.: Utilização do sensor AIRDAS (Airborne Infrared Disaster Assessment System) no monitoramento de desflorestamentos no norte do Estado do Mato Grosso - Brasil, in Simpósio Brasileiro de Sensoriamento Remoto, 9 (SBSR), edited by T. Krug, B. F. T. Rudorff, and U. M. de Freitas, pp. 1433–1442, INPE, São José dos Campos., 1998.

Bayram, S., Ocal, M. E., Laptali Oral, E. and Atis, C. D.: Comparison of multi layer perceptron (MLP) and radial basis function (RBF) for construction cost estimation: the case of Turkey, J. Civ. Eng. Manag., https://doi.org/10.3846/13923730.2014.897988, 2016.

https://doi.org/10.5194/acp-2019-167
Preprint. Discussion started: 7 June 2019

Atmospheric Chemistry and Physics Discussions

Bishop, C. M.: Neural networks: a pattern recognition perspective, Neural Networks, https://doi.org/10.1.1.46.8742, 1996.

Black, K., Davis, P., Lynch, P., Jones, M., McGettigan, M. and Osborne, B.: Long-term trends in solar irradiance in Ireland and their potential effects on gross primary productivity, Agric. For. Meteorol., https://doi.org/10.1016/j.agrformet.2006.09.005, 2006.

Borma, L. S., da Rocha, H. R., Cabral, O. M., von Randow, C., Collicchio, E., Kurzatkowski, D., Brugger, P. J., Freitas, H., Tannus, R., Oliveira, L., Rennó, C. D. and Artaxo, P.: Atmosphere and hydrological controls of the evapotranspiration over a floodplain forest in the Bananal Island region, Amazonia, J. Geophys. Res., 114(G1), G01003, https://doi.org/10.1029/2007JG000641, 2009.

Bosveld, F. C. and Beljaars, A. C. M.: The impact of sampling rate on eddy-covariance flux estimates, Agric. For. Meteorol., 109(1), 39–45, https://doi.org/10.1016/S0168-1923(01)00257-X, 2001.

Boucher, O., Randall, D., Artaxo, P., Bretherton, C., Feingold, G., Forster, P., Kerminen, V.-M. V.-M., Kondo, Y., Liao, H., Lohmann, U., Rasch, P., Satheesh, S. K., Sherwood, S., Stevens, B., Zhang, X. Y. and Zhan, X. Y.: Clouds and Aerosols, Clim. Chang. 2013 Phys. Sci. Basis. Contrib. Work. Gr. I to Fifth Assess. Rep. Intergov. Panel Clim. Chang., https://doi.org/10.1017/CBO9781107415324.016, 2013.

Chin, M., Ginoux, P., Kinne, S., Torres, O., Holben, B. N., Duncan, B. N., Martin, R. V., Logan, J. a., Higurashi, A. and Nakajima, T.: Tropospheric Aerosol Optical Thickness from the GOCART Model and Comparisons with Satellite and Sun Photometer Measurements, J. Atmos. Sci., https://doi.org/10.1175/1520-0469(2002)059<0461:TAOTFT>2.0.CO;2, 2002.

Doughty, C. E., Flanner, M. G. and Goulden, M. L.: Effect of smoke on subcanopy shaded light, canopy temperature, and carbon dioxide uptake in an Amazon rainforest, Global Biogeochem. Cycles, 24(3), n/a-n/a, https://doi.org/10.1029/2009GB003670, 2010.

Ezhova, E., Ylivinkka, I., Kuusk, J., Komsaare, K., Vana, M., Krasnova, A., Noe, S., Arshinov, M., Belan, B., Park, S.-B., Lavrič, J. V., Heimann, M., Petäjä, T., Vesala, T., Mammarella, I., Kolari, P., Bäck, J., Rannik, Ü., Kerminen, V.-M. and Kulmala, M.: Direct effect of aerosols on solar radiation and gross primary production in boreal and hemiboreal forests, Atmos. Chem. Phys., 18(24), 17863–17881, doi:10.5194/acp-18-17863-2018, 2018.

Fletcher, C. G., Kravitz, B. and Badawy, B.: Quantifying uncertainty from aerosol and atmospheric parameters and their impact on climate sensitivity, Atmos. Chem. Phys., 18(23), 17529–17543, doi:10.5194/acp-18-17529-2018, 2018.

Forster, P., Ramaswamy, V., Artaxo, P., Berntsen, T., Betts, R., Fahey, D. W., Haywood, J., Lean, J., Lowe, D. C., Myhre, G., Nganga, J., Prinn, R., Raga, G., Schulz, M. and Van Dorland, R.: Changes in Atmospheric Constituents and in Radiative Forcing, in Climate Change 2007: The Physical Science Basis. Contribution of Working Group I to the Fourth Assessment Report of the Intergovernmental Panel on Climate Change., 2007.

He, J., Glotfelty, T., Yahya, K., Alapaty, K. and Yu, S.: Does temperature nudging overwhelm aerosol radiative

effects in regional integrated climate models?, Atmos. Environ., 154, 42–52, doi:10.1016/j.atmosenv.2017.01.040, 2017.

Henyey, L. C. and Greenstein, J. L.: Diffuse radiation in the Galaxy, Astrophys. J., 93, 70, https://doi.org/10.1086/144246, 1941.

Hubanks, P. A.: MODIS Atmosphere QA Plan for Collection 005, 57, 2012.

Kanniah, K. D., Beringer, J., North, P. and Hutley, L.: Control of atmospheric particles on diffuse radiation and terrestrial plant productivity: A review, Prog. Phys. Geogr., https://doi.org/10.1177/0309133311434244, 2012.

Kiehl, J. T. and Trenberth, K. E.: Earth's Annual Global Mean Energy Budget, Bull. Am. Meteorol. Soc., https://doi.org/10.1175/1520-0477(1997)078<0197:EAGMEB>2.0.CO;2, 1997.

Levy, R. C., Leptoukh, G. G., Kahn, R., Zubko, V., Gopalan, A. and Remer, L. A.: A critical look at deriving monthly aerosol optical depth from satellite data, IEEE Trans. Geosci. Remote Sens., https://doi.org/10.1109/TGRS.2009.2013842, 2009.

Loveland, T. R. and Belward, A. S.: The IGBP-DIS global 1km land cover data set, DISCover: First results, Int. J. Remote Sens., 18(15), 3289–3295, https://doi.org/10.1080/014311697217099, 1997.

Malavelle, F. F., Haywood, J. M., Mercado, L. M., Folberth, G. A., Bellouin, N., Sitch, S. and Artaxo, P.: Studying the impact of biomass burning aerosol radiative and climate effects on the Amazon rainforest productivity with an Earth system model, Atmos. Chem. Phys., 19(2), 1301–1326, doi:10.5194/acp-19-1301-2019, 2019.

Mayer, B. and Kylling, A.: Technical note: The libRadtran software package for radiative transfer calculations - description and examples of use, Atmos. Chem. Phys., 5(7), 1855–1877, https://doi.org/10.5194/acp-5-1855-2005, 2005.

Mayer, B., Hoch, S. W. and Whiteman, C. D.: Validating the MYSTIC three-dimensional radiative transfer model with observations from the complex topography of Arizona's Meteor Crater, Atmos. Chem. Phys., https://doi.org/10.5194/acp-10-8685-2010, 2010.

Mercado, L. M., Bellouin, N., Sitch, S., Boucher, O., Huntingford, C., Wild, M. and Cox, P. M.: Impact of changes in diffuse radiation on the global land carbon sink., Nature, 458(7241), 1014–7, doi:10.1038/nature07949, 2009.

Moreira, D. S., Longo, K. M., Freitas, S. R., Yamasoe, M. A., Mercado, L. M., Rosário, N. E., Gloor, E., Viana, R. S. M., Miller, J. B., Gatti, L. V., Wiedemann, K. T., Domingues, L. K. G. and Correia, C. C. S.: Modeling the radiative effects of biomass burning aerosols on carbon fluxes in the Amazon region, Atmos. Chem. Phys., 17(23), 14785–14810, doi:10.5194/acp-17-14785-2017, 2017.

Niyogi, D., Chang, H. I., Saxena, V. K., Holt, T., Alapaty, K., Booker, F., Chen, F., Davis, K. J., Holben, B., Matsui, T., Meyers, T., Oechel, W. C., Pielke, R. A., Wells, R., Wilson, K. and Xue, Y.: Direct observations

of the effects of aerosol loading on net ecosystem CO2exchanges over different landscapes, Geophys. Res. Lett., https://doi.org/10.1029/2004GL020915, 2004.

Oliveira, P. H. F., Artaxo, P., Pires, C., De Lucca, S., Procópio, A., Holben, B., Schafer, J., Cardoso, L. F., Wofsy, S. C. and Rocha, H. R.: The effects of biomass burning aerosols and clouds on the CO_2 flux in Amazonia, in Tellus, Series B: Chemical and Physical Meteorology, vol. 59, pp. 338–349., 2007.

O'Sullivan, M., Rap, A., Reddington, C. L., Spracklen, D. V., Gloor, M. and Buermann, W.: Small global effect on terrestrial net primary production due to increased fossil fuel aerosol emissions from East Asia since the turn of the century, Geophys. Res. Lett., 43(15), 8060–8067, doi:10.1002/2016GL068965, 2016.

Papale, D. and Valentini, R.: A new assessment of European forests carbon exchanges by eddy fluxes and artificial neural network spatialization, Glob. Chang. Biol., https://doi.org/10.1046/j.1365-2486.2003.00609.x, 2003.

Persad, G. G. and Caldeira, K.: Divergent global-scale temperature effects from identical aerosols emitted in different regions, Nat. Commun., 9(1), 3289, doi:10.1038/s41467-018-05838-6, 2018.

Pierluissi, J. H. and Peng, G.-S.: New Molecular Transmission Band Models For LOWTRAN, Opt. Eng., https://doi.org/10.1117/12.7973523, 1985.

Reindl, D. T., Beckman, W. A. and Duffie, J. A.: Evaluation of hourly tilted surface radiation models, Sol. Energy, 45(1), 9–17, https://doi.org/10.1016/0038-092X(90)90061-G, 1990.

Ricchiazzi, P., Yang, S., Gautier, C. and Sowle, D.: SBDART: A Research and Teaching Software Tool for Plane-Parallel Radiative Transfer in the Earth's Atmosphere, Bull. Am. Meteorol. Soc., 79(10), 2101–2114, https://doi.org/10.1175/1520-0477(1998)079<2101:SARATS>2.0.CO;2, 1998.

Roderick, M. L., Farquhar, G. D., Berry, S. L. and Noble, I. R.: On the direct effect of clouds and atmospheric particles on the productivity and structure of vegetation, Oecologia, 129(1), 21–30, doi:10.1007/s004420100760, 2001.

do Rosário, N. E., Yamasoe, M. A. and Longo, K. M.: Aerosol Optical Depth and Ångström Coefficient retrievals over the Amazon Forest during 2007 biomass burning season, 494–497., https://doi.org/10.1063/1.3117029, 2009.

do Rosário, N. E., Yamasoe, M. A., Brindley, H., Eck, T. F. and Schafer, J.: Downwelling solar irradiance in the biomass burning region of the southern Amazon: Dependence on aerosol intensive optical properties and role of water vapor, J. Geophys. Res. Atmos., https://doi.org/10.1029/2011JD015956, 2011.

Seinfeld, J. H. and Pandis, S. N.: Atmospheric Chemistry and Physics: From Air Pollution to Climate Change., 2006.

Song, X.-P., Huang, C., Saatchi, S. S., Hansen, M. C. and Townshend, J. R.: Annual Carbon Emissions from Deforestation in the Amazon Basin between 2000 and 2010, edited by B. Hérault, PLoS One, 10(5), e0126754, https://doi.org/10.1371/journal.pone.0126754, 2015.

https://doi.org/10.5194/acp-2019-167
Preprint. Discussion started: 7 June 2019

Atmospheric Chemistry and Physics Discussions

Stanhill, G. and Cohen, S.: Global dimming: a review of the evidence for a widespread and significant reduction in global radiation with discussion of its probable causes and possible agricultural consequences, Agric. For. Meteorol., 107(4), 255–278, https://doi.org/10.1016/S0168-1923(00)00241-0, 2001.

Steiner, A. L., Mermelstein, D., Cheng, S. J., Twine, T. E. and Oliphant, A.: Observed Impact of Atmospheric Aerosols on the Surface Energy Budget, Earth Interact., 17(14), 1–22, doi:10.1175/2013EI000523.1, 2013.

Tang, H. and Dubayah, R.: Light-driven growth in Amazon evergreen forests explained by seasonal variations of vertical canopy structure, Proc. Natl. Acad. Sci., https://doi.org/10.1073/pnas.1616943114, 2017.

Textor, C., Schulz, M., Guibert, S., Kinne, S., Balkanski, Y., Bauer, S., Berntsen, T., Berglen, T., Boucher, O., Chin, M., Dentener, F., Diehl, T., Easter, R., Feichter, H., Fillmore, D., Ghan, S., Ginoux, P., Gong, S., Grini, A., Hendricks, J., Horowitz, L., Huang, P., Isaksen, I., Iversen, T., Kloster, S., Koch, D., Kirkevåg, A., Kristjansson, J. E., Krol, M., Lauer, A., Lamarque, J. F., Liu, X., Montanaro, V., Myhre, G., Penner, J., Pitari, G., Reddy, S., Seland, Stier, P., Takemura, T. and Tie, X.: Analysis and quantification of the diversities of aerosol life cycles within AeroCom, Atmos. Chem. Phys., https://doi.org/10.5194/acp-6-1777-2006, 2006.

Unger, N., Yue, X. and Harper, K. L.: Aerosol climate change effects on land ecosystem services, Faraday Discuss., 200, 121–142, doi:10.1039/C7FD00033B, 2017.

Vourlitis, G. L., De Souza Nogueira, J., De Almeida Lobo, F., Sendall, K. M., De Paulo, S. R., Antunes Dias, C. A., Pinto, O. B. and De Andrade, N. L. R.: Energy balance and canopy conductance of a tropical semi-deciduous forest of the southern Amazon Basin, Water Resour. Res., https://doi.org/10.1029/2006WR005526, 2008.

Wang, Y., Wang, M., Zhang, R., Ghan, S. J., Lin, Y., Hu, J., Pan, B., Levy, M., Jiang, J. H. and Molina, M. J.: Assessing the effects of anthropogenic aerosols on Pacific storm track using a multiscale global climate model, Proc. Natl. Acad. Sci., 111(19), 6894–6899, doi:10.1073/pnas.1403364111, 2014.

Whitley, R. J., Macinnis-Ng, C. M. O., Hutley, L. B., Beringer, J., Zeppel, M., Williams, M., Taylor, D. and Eamus, D.: Is productivity of mesic savannas light limited or water limited? Results of a simulation study, Glob. Chang. Biol., https://doi.org/10.1111/j.1365-2486.2011.02425.x, 2011.

Yamasoe, M. A., Von Randow, C., Manzi, A. O., Schafer, J. S., Eck, T. F. and Holben, B. N.: Effect of smoke and clouds on the transmissivity of photosynthetically active radiation inside the canopy, Atmos. Chem. Phys., https://doi.org/10.5194/acp-6-1645-2006, 2006.

Zhang, M., Yu, G. R., Zhang, L. M., Sun, X. M., Wen, X. F., Han, S. J. and Yan, J. H.: Impact of cloudiness on net ecosystem exchange of carbon dioxide in different types of forest ecosystems in China, Biogeosciences, https://doi.org/10.5194/bg-7-711-2010, 2010.

https://doi.org/10.5194/acp-2019-167
Preprint. Discussion started: 7 June 2019

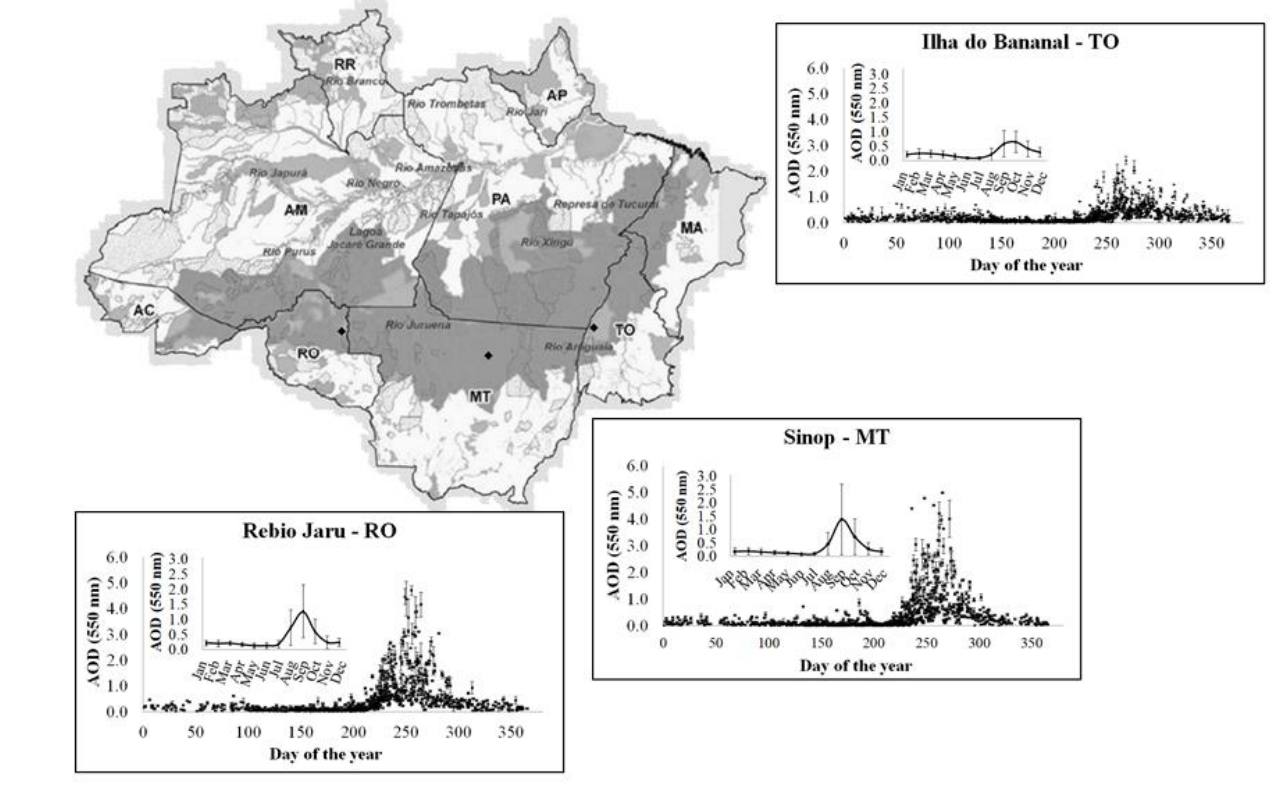

Figure 1: Geographical representation of the North region of Brazil. The darker gray area represents the deforestation arch of the Brazilian Amazon. The black dots indicate the location of the study sites: Rebio Jaru, RO, Sinop, MT, and Bananal Island, TO. Boxes show the temporal distribution of the aerosol optical depth at 550 nm over the three sites derived from MODIS from 2003 and 2008 and the monthly mean values for the period, with the standard deviation represented by vertical bars.

https://doi.org/10.5194/acp-2019-167
Preprint. Discussion started: 7 June 2019

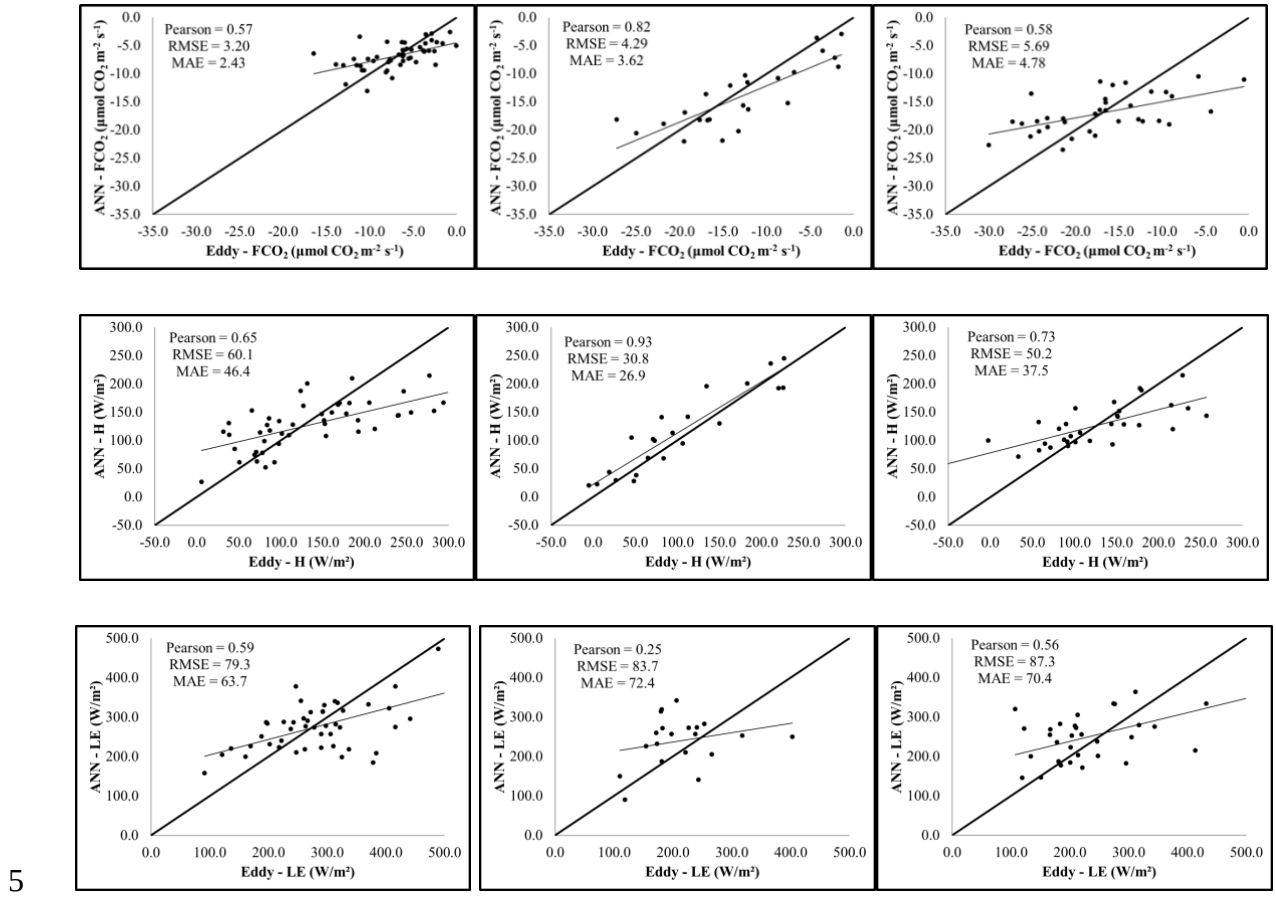

a. Bananal Island - TO **b. Rebio Jaru - RO** **c. Sinop – MT**

Figure 2: FCO_2 (µmol CO_2 $m^{-2}s^{-1}$), H (W/m^2), and LE (W/m^2) calculated from flux tower data through eddy covariance (x-axis) versus modelled by ANNs (y-axis), with Pearson coefficient, RMSE, and MAE. The 1:1 straight line (thick) and the linear fit (thin) are also represented for the three study sites.

https://doi.org/10.5194/acp-2019-167
Preprint. Discussion started: 7 June 2019

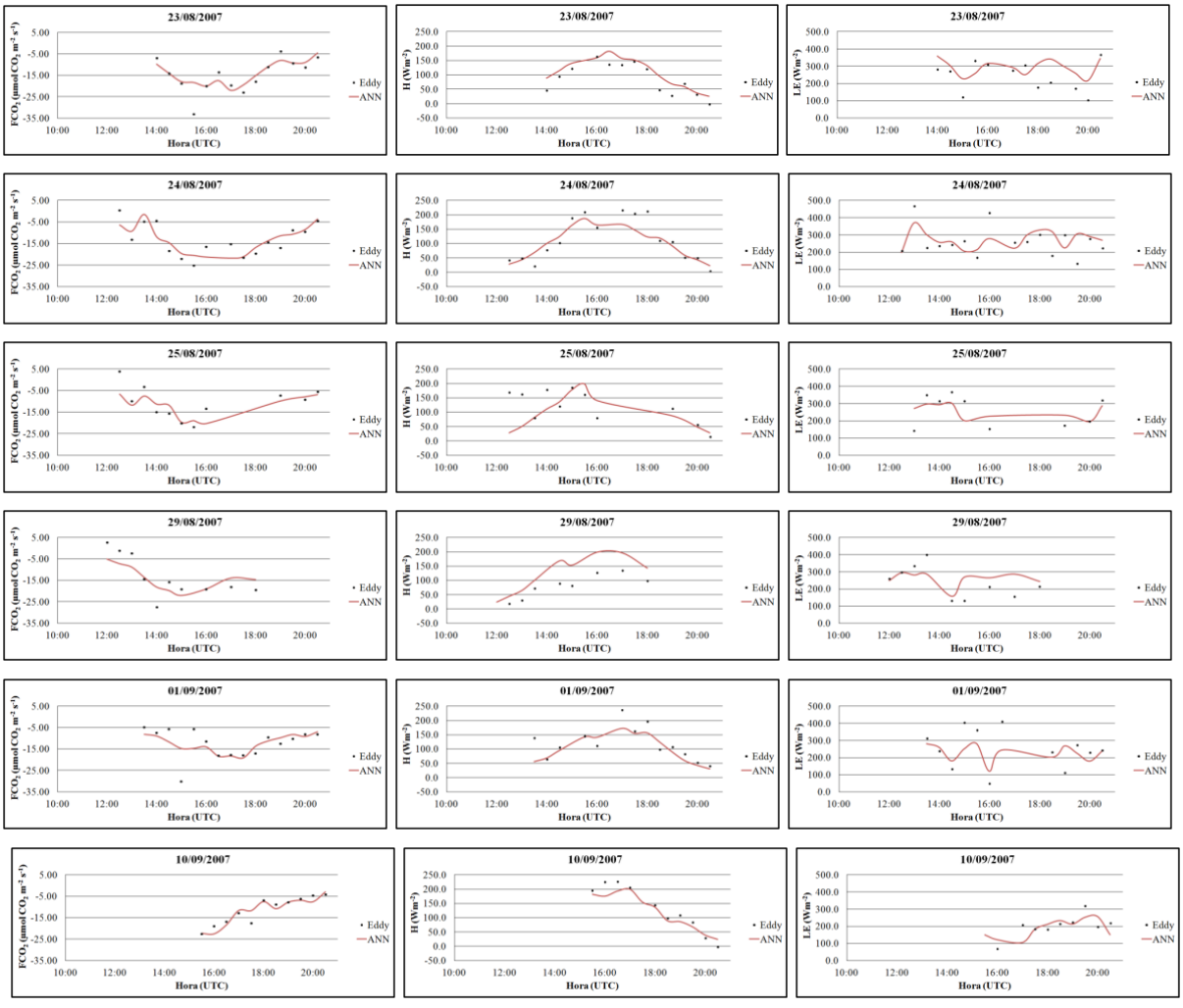

Figure 3. Diurnal cycle of FCO_2 (μmol CO_2 $m^{-2}s^{-1}$), H (W/m^2), and LE (W/m^2) calculated from flux tower data through eddy covariance (black dots) and modelled by ANNs (red line) for 6 days (23rd Aug, 24th Aug, 25th Aug, 29th Aug, 01st Sep, and 10th Sep) over the dry season of 2007 in Rebio Jaru.

https://doi.org/10.5194/acp-2019-167
Preprint. Discussion started: 7 June 2019

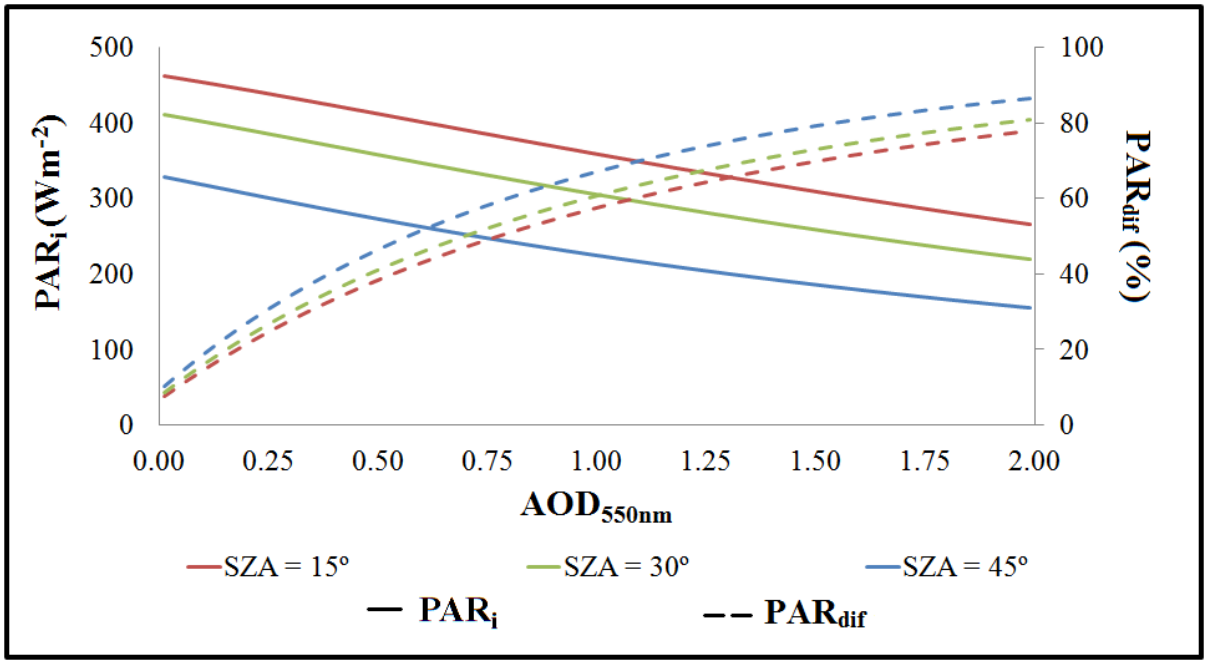

Figure 4: PARi (Wm^{-2}) (continuous lines) and PAR*dif* (%) (dashed lines) versus AOD550nm, for three different SZAs (15°, 30°, and 45°) calculated by the radiative transfer model, libRadtran, for Bananal Island for a characteristic day of the dry season.

https://doi.org/10.5194/acp-2019-167
Preprint. Discussion started: 7 June 2019

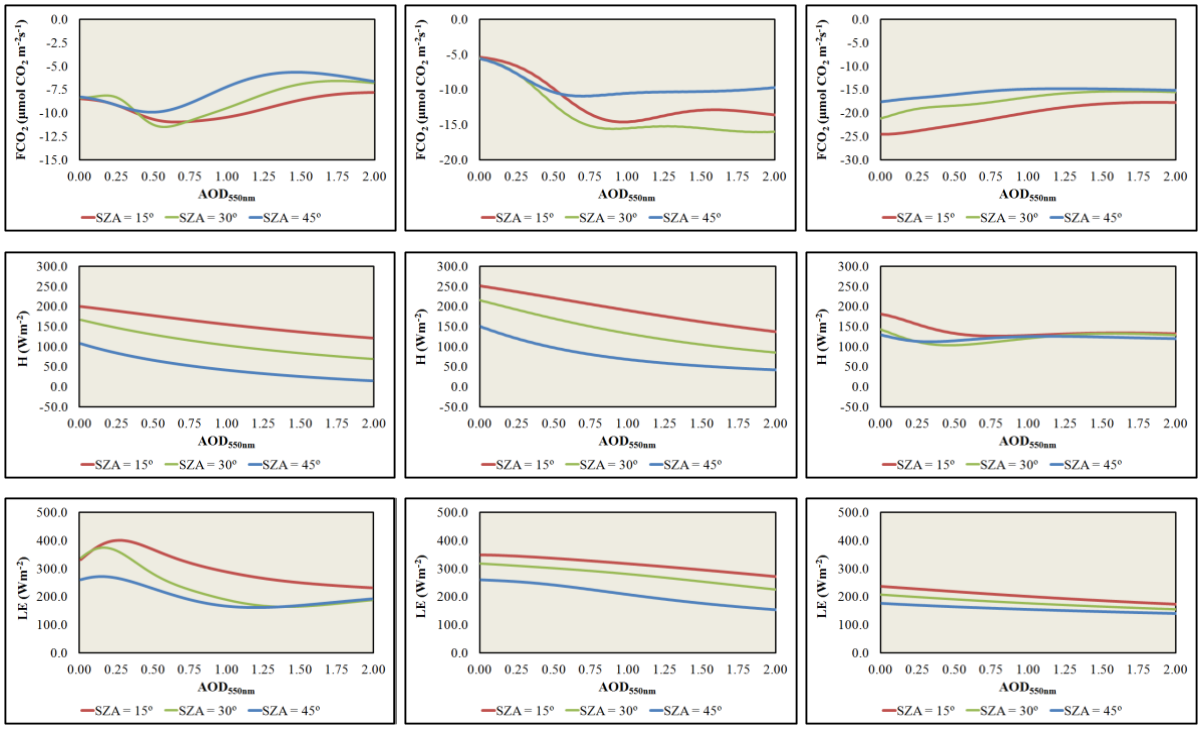

a. Bananal Island - TO **b. Rebio Jaru - RO** **c. Sinop - MT**

Figure 5: Modelled FCO_2 (µmol CO_2 $m^{-2}s^{-1}$), H (W/m^2), and LE (W/m^2) via ANNs versus AOD_{550nm}, for three SZAs (15°, 30°, and 45°), for three study sites. Values of temperature, VPD, and u* were kept constant. PAR_i and PAR_{dif} were obtained through *libRadtran*.

https://doi.org/10.5194/acp-2019-167
Preprint. Discussion started: 7 June 2019

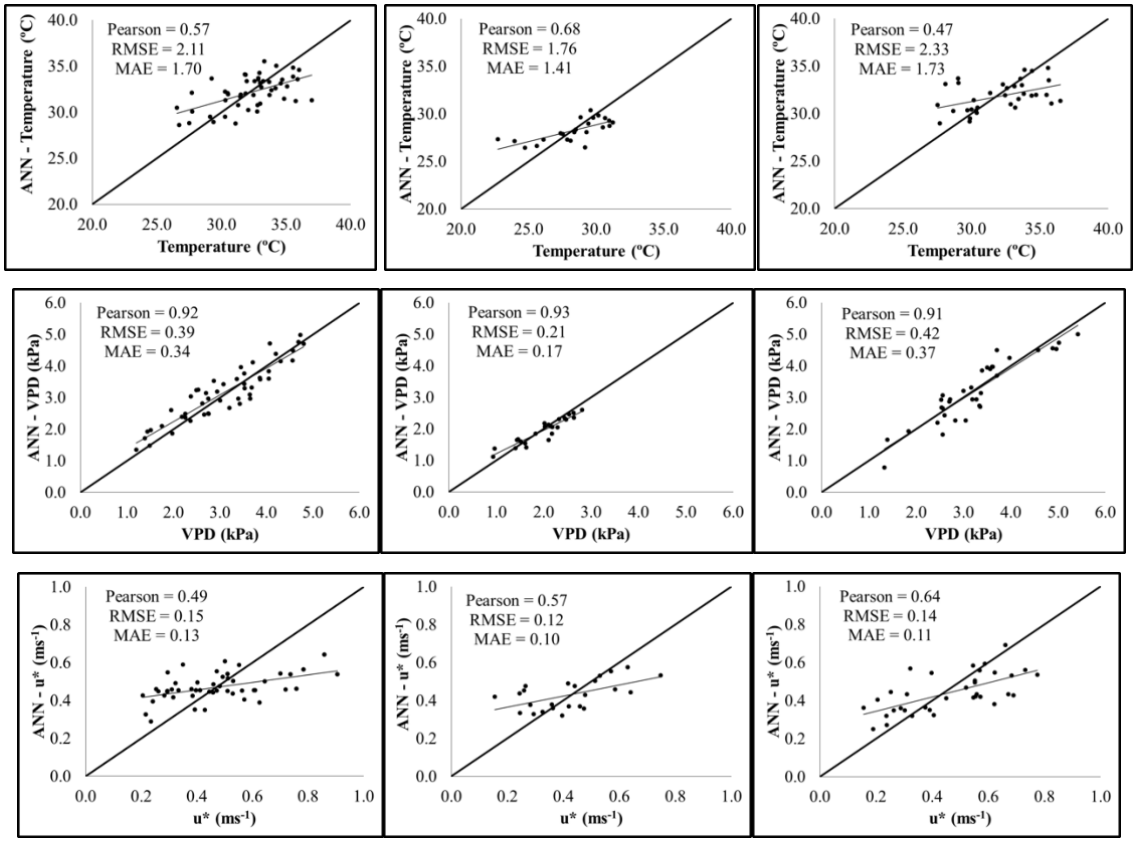

a. Bananal Island - TO **b. Rebio Jaru - RO** **c. Sinop – MT**

Figura 6: Temperature (°C), VPD (kPa), and u* (m.s^{-1}) obtained from ANNs generated with observed values for the three study sites, with respective Pearson coefficient, MAE, and RMSE. The 1: 1 line (thick) and the best linear fit (thin) are also shown.

https://doi.org/10.5194/acp-2019-167
Preprint. Discussion started: 7 June 2019

Atmospheric Chemistry and Physics Discussions

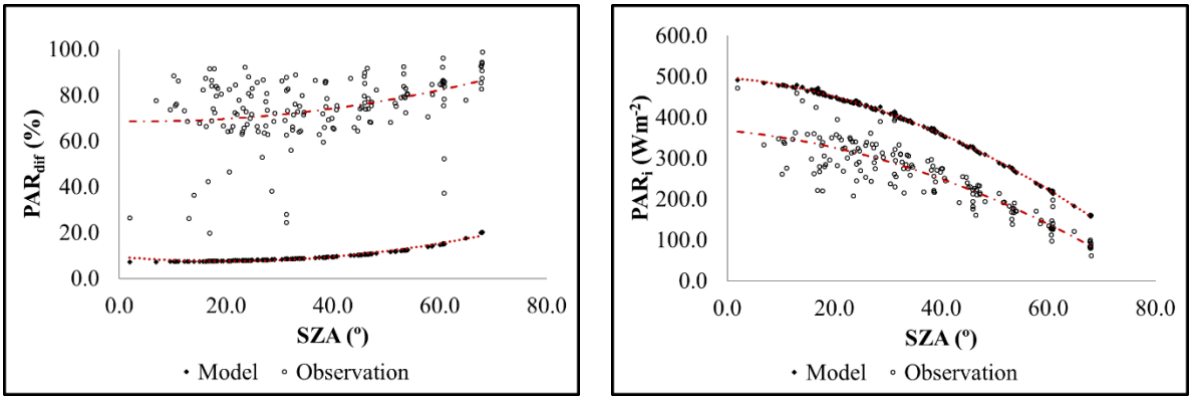

Figure 7: PAR_i (Wm^{-2}) (left) and PAR_{dif} (%) (right) versus SZA (°), for Rebio Jaru. The observed values of PAR_i and PARdif - obtained by the method of Reindl (1990) - are represented by open circles, while the values calculated through libRadtran are represented by the black dots. The curves fitted to the data sets are shown in red.

https://doi.org/10.5194/acp-2019-167
Preprint. Discussion started: 7 June 2019

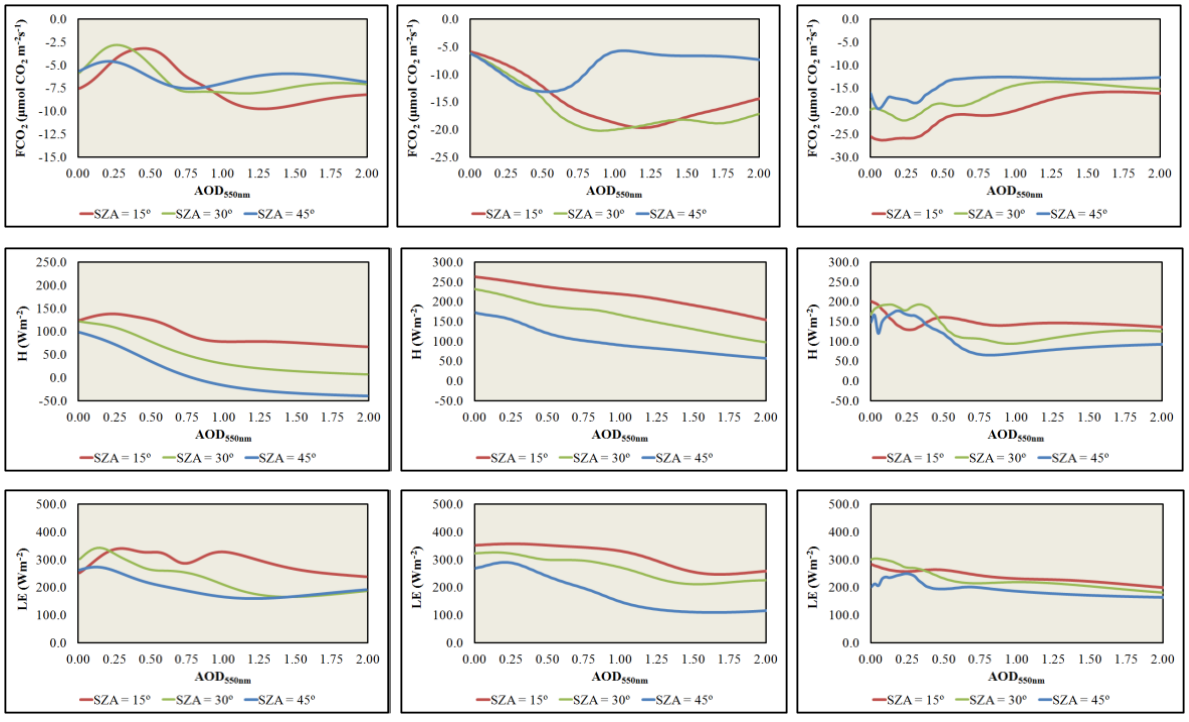

a. Bananal Island - TO **b. Rebio Jaru - RO** **c. Sinop - MT**

Figure 8: Modelled FCO2 (µmol CO2 m-2s-1), H (W/m²), and LE (W/m²) via ANNs versus AOD550nm, for three SZAs (15°, 30°, and 45°), for three study sites. Values of temperature, VPD, and u* were statistically modelled with ANNs built from meteorological data. PARi and PARdif were obtained through libRadtran.

https://doi.org/10.5194/acp-2019-167
Preprint. Discussion started: 7 June 2019

Atmospheric Chemistry and Physics Discussions

Table 1: Geographic coordinates, altitudes, flux tower height, and the sensors used in the three experimental sites.

	Bananal Island	Rebio Jaru	Sinop
Coordinates	9°49.3'S; 50°08.9'W	10°04.7'S; 61°56.0'W	11°24.7'S; 55°19.4'W
Altitude	120 m	148 m	423 m
Flux tower height	40 m	62 m	40 m
Period	Oct/2003 - Dec/2008	Aug/2007 - Oct/2007	Mar/2005 - Aug/2008
datalogger	CR5000 & CR10X (Campbell Sci.)	CR10X (Campbell Sci.)	CR5000 & CR10X (Campbell Sci.)
		Fluxes	
Sonic anemometer	CSAT3; 10 Hz	Solent 1012R2; 10.4Hz	SWS-211/3K; 10 Hz
Gas analyser	IRGA, Li-7500	IRGA, Li-7500	NOAA-ATDD
		Meteorological variables	
Temperature and humidity	Psychrometer CSI HMP45C	Termohygrometer Vaisala (HMP45D)	HMP-35 Vaisala
Precipitation	Hydrological Services	Pluviometer EM ARG-100	2501, Sierra-Misco
Net radiation	Net radiometer (Kipp&Zonen)	Net radiometer (Kipp&Zonen)	NR-LITE (Kipp&Zonen)
		Radiation	
Solar radiation	Pyranometer (Kipp&Zonen)	CM-21 (Kipp&Zonen)	*libRadtran*[1]
PAR	Radiometer (Kipp&Zonen)	Skye SKE-150	*libRadtran*[1]
		Aerosol	
AOD_{550nm}	MODIS	MFRSR[2]	MODIS

[1] Values obtained from the radiative transfer model
[2] *Multi-Filter Rotating Shadowband Radiometer*

Table 2: Fixed values of temperature (T), vapor pressure deficit (VPD), and friction velocity (u*) for three sites evaluated in the first test.

	Bananal Island - TO	Rebio Jaru - RO	Sinop - MT
T (ºC)	28.5	29.0	29.0
VPD (kPa)	1.5	2.0	2.0
u* ($m.s^{-1}$)	0.3	0.2	0.2

https://doi.org/10.5194/acp-2019-167
Preprint. Discussion started: 7 June 2019

Atmospheric Chemistry and Physics Discussions

Table 3: Mean values with standard deviations of the turbulent fluxes of CO_2 (FCO_2), sensible heat (H), and latent heat (LE), in µmol CO_2 $m^{-2}s^{-1}$ and Wm^{-2}, respectively. These values were used as input parameters for building ANNs (Measured), mean values and standard deviations generated from the aerosol free scenarios (Modelled), and relative differences (%) between the measured and the modelled values for all three study sites.

Study site	Variables	Measured	Modelled	Relative difference
Bananal Island - TO	FCO_2	-7.0 ± 5.0	-6.2 ± 0.7	+12.4%
	H (Wm^{-2})	130.9 ± 66.8	346.6 ± 111.7	+62.2%
	LE (Wm^{-2})	286.9 ± 107.9	305.9 ± 26.3	+6.2%
Rebio Jaru - RO	FCO_2	-12.2 ± 7.1	-5.5 ± 0.2	+55.3%
	H (Wm^{-2})	117.4 ± 73.6	183.7 ± 65.3	+36.1%
	LE (Wm^{-2})	215.4 ± 97.7	219.1 ± 69.7	+1.7%
Sinop - MT	FCO_2	-17.5 ± 7.4	-19.7 ± 2.7	-12.4%
	H (Wm^{-2})	138.6 ± 70.7	162.0 ± 23.7	+14.5%
	LE (Wm^{-2})	227.2 ± 88.6	262.0 ± 38.3	+13.3%